PARAMETRIC STUDIES OF THE NSM FRP STRIPS SHEAR STRENGTH CONTRIBUTION TO A RC BEAM

Vincenzo Bianco, J.A.O. Barros and Giorgio Monti

Synopsis: A three dimensional mechanical model was recently developed to simulate the shear strength contribution provided by a system of Near Surface Mounted (NSM) Fiber Reinforced Polymer (FRP) strips to a Reinforced Concrete (RC) beam throughout its loading process. It was developed fulfilling equilibrium, kinematic compatibility and constitutive laws of both materials, concrete and FRP, and local bond between themselves. In the present paper, that model is first appraised on the basis of some of the most recent experimental results and then is applied to carry out parametric studies. The influence of each of the involved parameters on the contribution provided by a system of NSM FRP strips to the shear strength of a RC beam is investigated. The results of those studies are presented along with the main findings.

Keywords: Numerical Model; FRP; NSM; Shear Strengthening; Concrete Fracture; Debonding; Tensile Rupture, Parametric Studies.

Vincenzo Bianco is a Post Doc at the Department of Structural Engineering and Geotechnics of the Sapienza University of Rome, Italy. He received his PhD from the Sapienza University of Rome. His research interests include seismic assessment and retrofit of existing structures, mechanical modeling and use of composite materials for structural rehabilitation.

Joaquim Barros is an Associate Professor with aggregation and Director of the Laboratory of the Structural Group of the Department of Civil Engineering, University of Minho at Guimarães, Portugal. He received his MSc and PhD from the University of Porto, Portugal. He is a member of ACI Committees 440 and 544, and fib TG 8.3 and 9.3. His research interests include structural strengthening, composite materials, fiber reinforced concrete and finite element method.

Giorgio Monti is a Full Professor at the Department of Structural Engineering and Geotechnics of the Sapienza University of Rome, Italy. He received is MSc from the University of Berkley, California, and his PhD from the Sapienza University of Rome. His Research interests span from reliability to the assessment and retrofitting of existing structures in seismic zones.

INTRODUCTION

Shear strengthening of RC beams by NSM technique consists in gluing FRP strips by an adhesive into thin shallow slits cut onto the concrete cover of the beam web lateral faces. Recent findings (Bianco *et al.* 2006-2007a) have spotlighted that the failure modes that can affect the behavior, at ultimate, of a NSM FRP strip subject to an imposed end slip comprise, depending on the relative mechanical and geometrical properties of the materials involved: debonding, tensile rupture of the strip, concrete semi-conical tensile fracture and a mixed shallow-semi-cone-plus-debonding failure mode (Fig. 1a). The term *debonding* is adopted to designate loss of bond due to damage initiation and propagation within the adhesive layer and at the FRP strip-adhesive and adhesive-concrete interfaces, so that the strip pulling out results (Fig. 1a).

When principal tensile stresses transferred to the surrounding concrete attain its tensile strength, concrete fractures along a surface, envelope of the compression isostatics, whose shape can be conveniently assumed as semi-conical (Fig. 1a). Increasing the imposed end slip, subsequent coaxial semi-conical fracture surfaces can occur in the concrete surrounding the NSM strip that progressively reduce the resisting bond length *i.e.* the portion of the initial bond length still adhered to concrete. Those subsequent fractures can either progress up to the free end, resulting in a *concrete semi-conical failure*, or stop progressing midway between loaded and free end, resulting in a *mixed-shallow-semi-cone-plus-debonding* failure (Fig. 1a). Moreover, regardless of an initial concrete fracture, the strip can *rupture* (Fig. 1a). During the loading process of a RC beam subject to shear, when concrete average tensile strength f_{ctm} is exceeded at the web intrados, some shear cracks originate therein and successively progress towards the web extrados. Those cracks can be thought as a single Critical Diagonal Crack (CDC) inclined of an angle θ with respect to the beam longitudinal axis (Fig. 1b). The CDC can be schematized as an inclined plane dividing the web into two portions sewn together by the crossing strips (Fig. 1b).

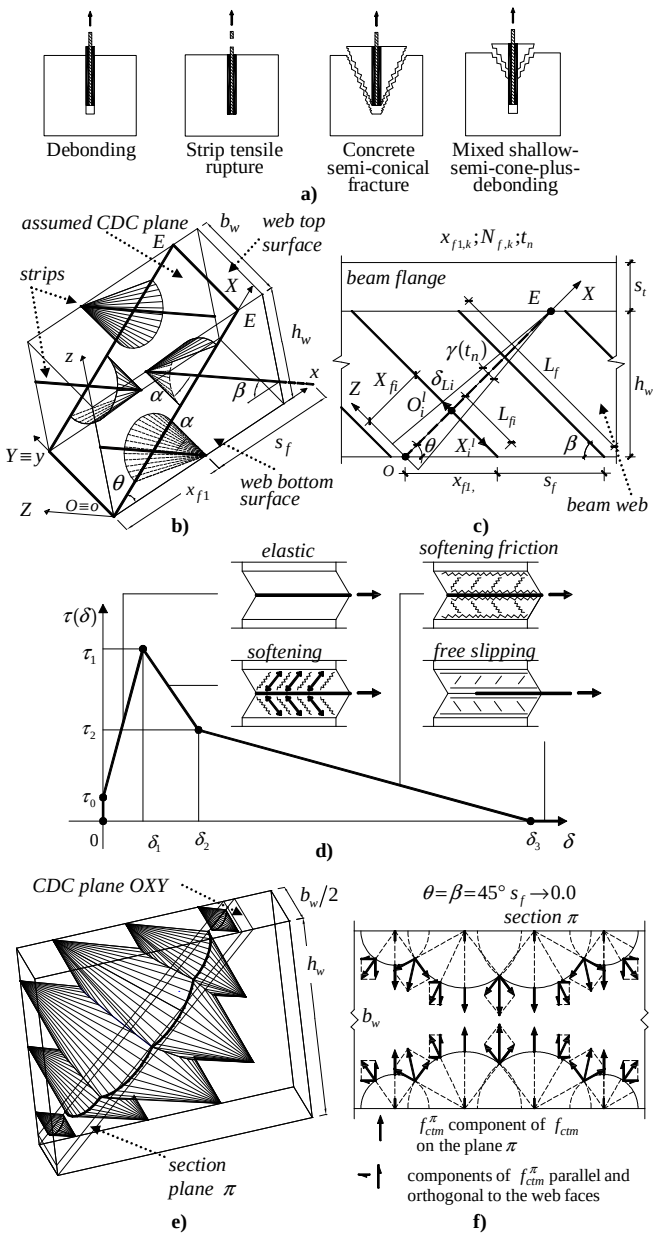

Figure 1 — Main features of the mechanical behavior of NSM FRP strips for shear strengthening of RC beams: a) failure modes of a NSM strip subject to an increasing end slip, b) web schematization, c) loading process, d) local bond characteristics, e) interaction among adjacent strips and f) web section parallel to the CDC plane.

At load step t_1, the two web parts, separated by the CDC, start moving apart by pivoting around the crack end (line *E-E* in Fig. 1b-c). From that step on, by increasing the applied load, the CDC opening angle $\gamma(t_n)$ progressively widens (Fig. 1c). The strips crossing the CDC oppose its widening by anchoring to the surrounding concrete to which they transfer, by bond, the force originating at their intersection with the CDC, O_i^l, as a result of the imposed end slip $\delta_{Li}[\gamma(t_n)]$. The capacity of each strip is provided by its available bond length L_{fi} that is the shorter between the two parts into which the CDC divides its actual length L_f (Fig. 1c). Bond is the mechanism through which stresses are transferred to the surrounding concrete (Yuan *et al.* 2004, Mohammed Ali *et al.* 2006 and 2007). The subsequent phases undergone by bond during the loading process, representing the physical phenomena occurring in sequence within the adhesive layer by increasing the imposed end slip, are: "elastic", "softening", "softening friction" and "free slipping" (Fig. 1d) (Bianco *et al.* 2007b). The first rigid branch (0-τ_0) represents the overall initial shear strength of the joint, independent of the deformability of the adhesive layer and attributable to the micro-mechanical and, mainly, to chemical properties of the involved materials and relative interfaces. In fact, the parameter τ_0 is the average of the following physical entities encountered in sequence by stresses flowing from the strip to the surrounding concrete, *i.e.*: adhesion at the strip-adhesive interface, cohesion within the adhesive itself, and adhesion at the adhesive-concrete interface (*e.g.* Sekulic and Curnier 2006, Zhai *et al.* 2008). From τ_0 up to the peak strength τ_1, a macro-mechanical strength due to the elastic stiffness of the intact adhesive layer adds to the constant adhesive-cohesive strength. That macro-mechanical strength can be conveniently modeled by a linear elastic behavior. Approaching the peak strength, the adhesive fractures along diagonal planes orthogonal to the tension isostatics, as outlined also by Sena-Cruz and Barros (2004) by means of post-test optical microscope photos and nonlinear finite element analysis (Sena-Cruz 2004). During the subsequent *softening* phase (Fig. 1d), force is transferred from the strip to the surrounding concrete by the resulting diagonal micro-struts. Throughout the softening phase, by increasing the imposed slip, the extremities of those adhesive micro-struts progressively deteriorate so that micro-cracks parallel to the strip start to appear at both the strip-adhesive and adhesive-concrete interfaces. Approaching the *softening friction* phase (Fig. 1d), the softening resisting mechanism is gradually replaced by friction and micro-mechanical interlock along those micro-cracks. Nonetheless, even those mechanisms undergo softening due to progressive degradation. When the resisting force provided by friction is exhausted, those micro-cracks result in smooth discontinuities. The *free slipping* phase (Fig. 1d) follows, during which the strip keeps being pulled out without having to overcome any opposing restraint left. Reducing the spacing between subsequent strips s_f (Figs. 1b-c), their semi-conical fracture surfaces overlap and the resulting envelope area progressively becomes smaller than the mere summation of each of them (see Fig. 1e). That detrimental interaction between strips can be taken into account by modifying the semi-conical surface pertaining to each strip accordingly. By decreasing the strips spacing, the concrete fracture envelope surface is almost parallel to the web face of the beam, as confirmed in experimental observations reporting the detachment of

the concrete cover from the underlying beam core (*e.g.* Dias *et al.* 2007, Dias and Barros 2008, Rizzo and De Lorenzis 2009). Since the position of those semi-conical surfaces is symmetric with respect to the vertical plane passing through the beam axis, the horizontal outward components of the tensile strength vectors, distributed throughout their surfaces, are balanced only from an overall standpoint but not locally (Fig. 1f). That local unbalance of the horizontal tensile stress components, orthogonal to the beam web face, justifies the outward expulsion of the concrete cover in both the uppermost and lowermost parts of the strengthened sides of the web (Dias and Barros 2008, Rizzo and De Lorenzis 2009). Consistently with those mechanical principles, a comprehensive closed-form three-dimensional model for predicting the NSM shear strength contribution to a RC beam was recently developed (Bianco 2008, Bianco *et al.* 2009a-b and 2010). That model allows the NSM FRP strips shear strength contribution to be calculated for each value of the CDC opening angle $V_{f,k}[\gamma(t_n)]$ and for each *k*-th geometrical configuration that the occurred CDC could assume with respect to the system of NSM FRP strips. That model was implemented in a stand-alone C language computer program in order to carry out simulations of experimental data and to perform parametric studies. In the next sections, after a brief presentation of further analytical details, the results of a study regarding the influence of each parameter on the shear strength contribution provided by a system of NSM FRP strips to a RC beam are presented along with the main findings and implications.

RESEARCH SIGNIFICANCE

A model was developed to assess the influence of each of the intervening parameters on the shear strength contribution provided to a RC beam by a system of NSM strips. The obtained results evidence a gradual variation of both the prevailing ultimate behavior and corresponding configuration assumed by the system of NSM FRP strips. The outcomes of the studies presented are very useful to better understand the relative influence of the various input parameters on the ultimate behavior of the system of NSM FRP strips.

NSM FRP STRIPS' SHEAR STRENGTH CONTRIBUTION TO A RC BEAM: APPRAISAL

The proposed model was applied to a large amount of tested RC beams (Bianco *et al.* 2010) nonetheless, for the sake of brevity, only the results regarding some of the beams tested by Dias *et al.* (2007) are reported in the present paper. Those beams are characterized by the following common geometrical and mechanical parameters: $b_w = 180\ mm$; $h_w = 300\ mm$; $f_{cm} = 18.6\ MPa$; $f_{fu} = 2952\ MPa$; $E_f = 166\ GPa$; $a_f = 1.4\ mm$; $b_f = 10.0\ mm$ and $\beta = 45^o$ (1 *mm* = 0.0394 *in* - 1 *N* = 0.2248 *lb* - 1000 *psi* = 6.9 *MPa*). The parameters characterizing the adopted local bond stress-slip relationship are (Bianco *et al.* 2009b): $\tau_0 = 2.0\ MPa$; $\tau_1 = 20.1\ MPa$; $\tau_2 = 9.0\ MPa$; $\delta_1 = 0.07\ mm$; $\delta_2 = 0.83\ mm$; $\delta_3 = 14.1\ mm$. The CDC inclination angle θ adopted in the simulations plotted in Fig. 2 is the one experimentally observed $\theta^{\exp}$. The angle α was assumed equal to 28.5°, being the average of values obtained in a previous investigation (Bianco *et al.* 2006) by back-analysis of experimental data. The two parameters characterizing the loading process are: $\dot{\gamma} = 0.01°$ and $\gamma_{\max} = 0.6°$. Concrete

average tensile strength f_{ctm} was calculated from the average compressive strength by means of the formulae present in the CEB Fip Model Code 1990 resulting in 1.45 *MPa*. From the numerical/experimental comparison, a satisfactory predictive performance of the proposed model, in terms of peak NSM shear strength contribution $V_{f,k}^{\max}$, was obtained. In fact, for all the beams simulated, whose results (Bianco *et al.* 2010) are herein omitted for the sake of brevity, the experimental value always lies in between the minimum and maximum values of the numerical predictions and the ratios $V_{f,k}^{\min}/V_f^{\exp}$ and $V_{f,k}^{\max}/V_f^{\exp}$ are characterized by mean value and standard deviation $(\mu;\sigma)$ equal to $(0.99;0.59)$ and $(1.38;0.77)$, respectively.

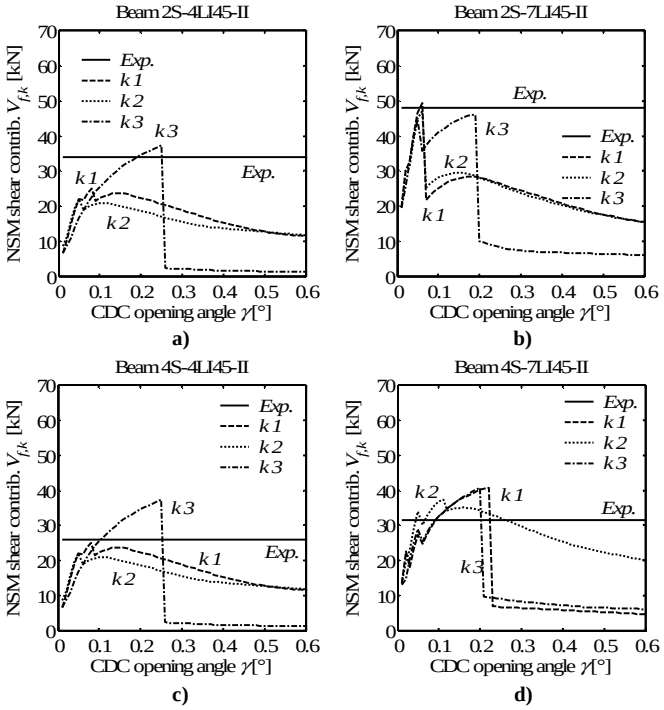

Figure 2 — NSM FRP strips' shear strength contribution to a RC beam. Appraisal of the proposed model for some of the beams tested by Dias *et al.* (2007): a) beam 2S-4LI45-II ($\theta^{\exp}=40^{\circ}$, $s_f=275\,mm$ and stirrups $\phi 6/300\,mm$); b) beam 2S-7LI45-II ($\theta^{\exp}=30^{\circ}$, $s_f=157\,mm$ and stirrups $\phi 6/300\,mm$); c) beam 4S-4LI45-II ($\theta^{\exp}=40^{\circ}$, $s_f=275\,mm$ and stirrups $\phi 6/180\,mm$); d) beam 4S-7LI45-II ($\theta^{\exp}=40^{\circ}$, $s_f=157\,mm$ and stirrups $\phi 6/180\,mm$) (1 *mm* = 0.0394 *in* - 1 *N* = 0.2248 *lb* - 1000 *psi* = 6.9 *MPa*).

The typical graph of the shear strength contribution as function of the CDC opening angle $V_f\,[\gamma(t_n)]$ is characterized by abrupt decays which correspond to the strips failure.

The peculiar behavior of a RC beam strengthened in shear by NSM technique can be easily explained referring to one of those beams, as for instance the beam labeled 2S-7LI45-II whose cracking scenario, both numerically predicted and experimentally recorded, is reported in Fig. 3.

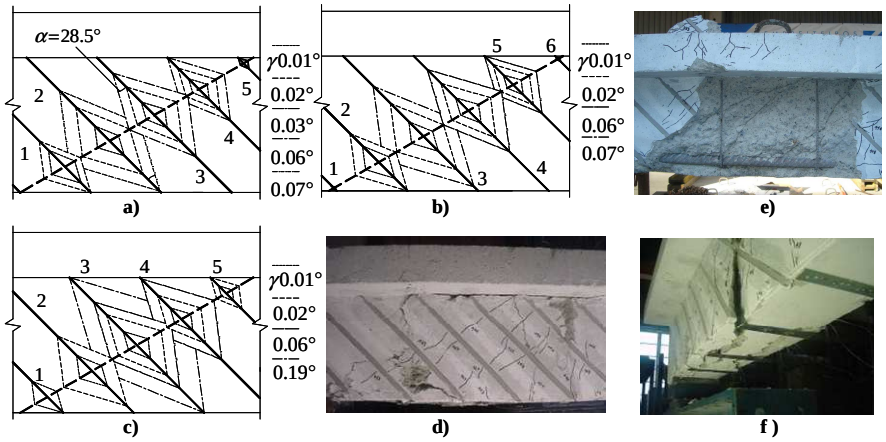

Figure 3 — Cracking scenario of the 2S-7LI45-II beam: numerical result for a) k = 1, b) k = 2, c) k = 3, and d-f) experimental post-test pictures.

Since the first load steps, concrete surrounding each of the strips fractures and concrete fracture, starting from the CDC plane, progressively penetrates inside the core of the beam web. The first strips to fail are those characterized by the shortest available bond lengths that generally fail in the first stages of the loading process, like for instance: the 1st ($\gamma = 0.02°$) and the 5th ($\gamma = 0.03°$) of the 1st configuration (Fig. 3a); the 1st and 6th ($\gamma = 0.01°$) and the 2nd ($\gamma = 0.02°$) of the 2nd configuration (Fig. 3b). Those failures are not so evident in the corresponding graph (Fig. 2b) since, in the first load steps, the contribution provided by the strips with a larger available bond length is still increasing and is relatively predominant. When a strip fails at a higher stage of the loading process, the corresponding larger decay in the shear strengthening contribution of the FRP system is much more evident. This happens, for instance, for the 2nd strip of the 1st configuration at $\gamma = 0.07°$, the 3rd strip of the 2nd configuration at $\gamma = 0.07°$ or the 3rd strip of the 3rd configuration at $\gamma = 0.19°$. These first two are mixed shallow-semi-cone-plus-debonding failures and the third is characterized by a semi-conical concrete fracture that reaches the free extremity. After those failures, the corresponding graphs, present a different trend: in the first two cases, a maximum relative follows while, in the third, the shear carrying capacity goes on diminishing in a continuous way. The former behavior is due to the fact that, when the last fracture occurs, that is the mixed failure of the 2nd and 3rd strip, respectively, the remaining strips still have a resisting bond length larger than the required transfer length and their contribution can still increase before gradual complete

debonding follows. The latter is due to the fact that, when the 3rd central strip fails, the 2nd and the 4th, had already failed by mixed failure so that the overall carrying capacity goes on diminishing up to the complete debonding of their left resisting bond lengths.
It has to be stressed that, since lateral strips characterized by the shortest values of the available bond length fail in the early stages of the loading process, the strips which significantly contribute to the peak NSM shear strength contribution $V_{f,k}^{\max}$, are the central ones.

PARAMETRIC STUDIES

The Reference Beam (RB) assumed for the parametric studies along with the range of values assumed for each parameter, are listed in Table 1. The values of the parameters characterizing the RB have been chosen in such a way to result approximately the average values of those that can be met in real practice. In some cases, the specific parameter is varied within a range that comprehends values a little beyond those having a strict physical confirmation, in order to assess not only their influence on the physical behavior of RC beams strengthened in shear by the NSM technique, but also their influence from a mere analytical/numerical standpoint. The range of variation of f_{cm} was limited to the values 10-90 *MPa* (Table 1) in order for concrete to be considered as *structural*, in accordance to the international regulations (*e.g.* CEB-FIP Model Code 1990).

The load step $\dot{\gamma}$ slightly influences, for the range of values in which it was herein varied (0.0001°-0.01°), the peak NSM shear strength contribution $V_{f,k}^{\max}$ (Fig. 4a). In this scenario, it is deemed reasonable to assume a value of the load step equal to $\dot{\gamma} = 0.01°$ since it guarantees a good compromise between accuracy of prediction and computational demand.

The peak NSM shear strength contribution $V_{f,k}^{\max}$ decreases by assuming increasing values of the CDC inclination angle θ since, other parameters being the same, the number of strips effectively crossing the CDC decreases (Fig. 4b).

The peak NSM shear strength contribution $V_{f,k}^{\max}$ increases by increasing the web cross section depth h_w (Fig. 4c), since both the number of strips effectively crossing the CDC and their available bond lengths increase in turn. For $h_w \le 400\,mm$ (1 *mm* = 0.0394 *in*), concrete fracture is so deep that: 1) the shorter lateral strips fail for semi-conical fracture and 2) the central longer ones fail for mixed-shallow-semi-cone-plus-debonding. For increasing values of h_w, concrete fracture progressively becomes shallower and the last values assumed by the resisting bond lengths increase. Therefore, since larger values of L_{Rfi} can attain larger values of peak bond-transferred force (Bianco 2008), $V_{f,k}^{\max}$ increases. For $h_w > 400\,mm$, after an initial and more superficial semi-conical fracture that involves all of the strips crossing the CDC, and the eventual failure of the shorter ones for mixed-shallow-semi-cone-plus-debonding, the central, longer ones, rupture. Thus, for increasing values of h_w, the larger the number of strips whose tensile strength can be attained, the larger the peak NSM shear strength contribution becomes.

Table 1 — Range of values of the parameters whose influence was investigated.

Study	$\dot{\gamma}$ °	θ °	h_w *mm*	b_w *mm*	a_f *mm*	b_f *mm*	s_f *mm*	β °	E_f *GPa*	f_{fu} *GPa*	f_{cm} *MPa*	α °	τ_0 *MPa*	τ_1 *MPa*	τ_2 *MPa*	δ_1 *mm*	δ_2 *mm*	δ_3 *mm*
RB	0.01	45.0	500.0	200.0	1.4	10.0	200.0	45.0	150.0	3.0	35.0	28.5	2.0	20.1	9.0	0.07	0.83	14.1
1	**1-10^{-4}**	45.0	500.0	200.0	1.4	10.0	200.0	45.0	150.0	3.0	35.0	28.5	2.0	20.1	9.0	0.07	0.83	14.1
2	0.01	**20-50**	500.0	200.0	1.4	10.0	200.0	45.0	150.0	3.0	35.0	28.5	2.0	20.1	9.0	0.07	0.83	14.1
3	0.01	45.0	**200-700**	200.0	1.4	10.0	200.0	45.0	150.0	3.0	35.0	28.5	2.0	20.1	9.0	0.07	0.83	14.1
4	0.01	45.0	500.0	**50-400**	1.4	10.0	200.0	45.0	150.0	3.0	35.0	28.5	2.0	20.1	9.0	0.07	0.83	14.1
5	0.01	45.0	500.0	200.0	**1.0-5.5**	10.0	200.0	45.0	150.0	3.0	35.0	28.5	2.0	20.1	9.0	0.07	0.83	14.1
6	0.01	45.0	500.0	200.0	1.4	**5-35**	200.0	45.0	150.0	3.0	35.0	28.5	2.0	20.1	9.0	0.07	0.83	14.1
7	0.01	45.0	500.0	200.0	1.4	10.0	**50-800**	45.0	150.0	3.0	35.0	28.5	2.0	20.1	9.0	0.07	0.83	14.1
8	0.01	45.0	500.0	200.0	1.4	10.0	200.0	**45-90**	150.0	3.0	35.0	28.5	2.0	20.1	9.0	0.07	0.83	14.1
9	0.01	45.0	500.0	200.0	1.4	10.0	200.0	45.0	**100-250**	3.0	35.0	28.5	2.0	20.1	9.0	0.07	0.83	14.1
10	0.01	45.0	500.0	200.0	1.4	10.0	200.0	45.0	150.0	**1.0-5**	35.0	28.5	2.0	20.1	9.0	0.07	0.83	14.1
11	0.01	45.0	500.0	200.0	1.4	10.0	200.0	45.0	150.0	3.0	**10-90**	28.5	2.0	20.1	9.0	0.07	0.83	14.1
12	0.01	45.0	500.0	200.0	1.4	10.0	200.0	45.0	150.0	3.0	35.0	**10-45**	2.0	20.1	9.0	0.07	0.83	14.1
13	0.01	45.0	500.0	200.0	1.4	10.0	200.0	45.0	150.0	3.0	35.0	28.5	**0.5-5**	20.1	9.0	0.07	0.83	14.1
14	0.01	45.0	500.0	200.0	1.4	10.0	200.0	45.0	150.0	3.0	35.0	28.5	2.0	**9.5-35**	9.0	0.07	0.83	14.1
15	0.01	45.0	500.0	200.0	1.4	10.0	200.0	45.0	150.0	3.0	35.0	28.5	2.0	20.1	**3.0-19**	0.07	0.83	14.1
16	0.01	45.0	500.0	200.0	1.4	10.0	200.0	45.0	150.0	3.0	35.0	28.5	2.0	20.1	9.0	**0.05-0.8**	0.83	14.1
17	0.01	45.0	500.0	200.0	1.4	10.0	200.0	45.0	150.0	3.0	35.0	28.5	2.0	20.1	9.0	0.07	**0.2-10**	14.1
18	0.01	45.0	500.0	200.0	1.4	10.0	200.0	45.0	150.0	3.0	35.0	28.5	2.0	20.1	9.0	0.07	0.83	**2.0-20**

(1 *mm* = 0.0394 *in* - 1 *N* = 0.2248 *lb* - 1000 *psi* = 6.9 *MPa*).

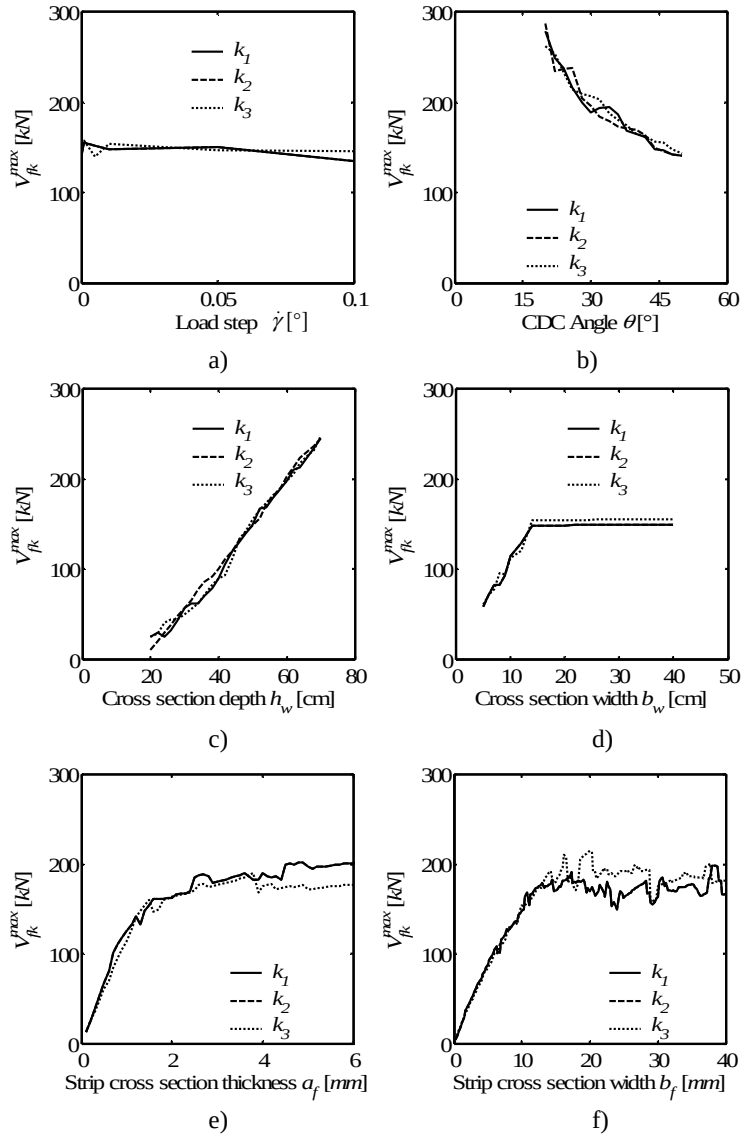

Figure 4 — Influence on the peak NSM shear strength contribution $V_{f,k}^{\max}$ of: a) load step $\dot{\gamma}$; b) CDC inclination angle θ; c) beam cross section depth h_w and d) width b_w; e) strip cross section thickness a_f and f) width b_f (1 *mm* = 0.0394 *in* - 1 *N* = 0.2248 *lb*).

By increasing the RC beam web cross section width b_w (Fig. 4d), the peak NSM shear strength contribution $V_{f,k}^{\max}$ presents a two-phases behavior with an almost clear-cut

division between themselves in correspondence of a value of approximately $b_w = 150\ mm$ (1 *mm* = 0.0394 *in*). For values of the web width $b_w \le 150\ mm$, by increasing b_w, $V_{f,k}^{\max}$ increases almost linearly up to a maximum while, for values of the web width $b_w > 150\ mm$, any further increase of b_w does not yield any further increase of $V_{f,k}^{\max}$. This is due to the fact that, for $b_w < 150\ mm$, the strips symmetrically placed on the opposite sides of the strengthened web interact transversally with each other, thus affecting the concrete semi-conical fracture capacities V_{fi}^{cf}. It follows that, for very short values of b_w, concrete semi-conical fracture is very deep and most of the strips effectively crossing the CDC fail since concrete fracture reaches their free extremity.

By increasing b_w, for values approaching $b_w = 150\ mm$, concrete fracture progressively becomes more superficial so that the last values assumed by the strips' resisting bond lengths and, consequently, the maximum force they can transfer by bond $V_{fi}^{bd,\max}$, increase. Thus, $V_{f,k}^{\max}$ increases linearly up to attaining its maximum for $b_w = 150\ mm$ in correspondence of which the last values of the resisting bond lengths of the central strips reach such values that allow them to transfer a maximum bond force $V_{fi}^{bd,\max}$ large enough to attain the strip rupture capacity V_f^{tr}. Therefore, for $b_w = 150\ mm$, central strips rupture. For values of $b_w > 150\ mm$, due to the lack of interaction between strips placed on the opposite sides of the beam web, any further increase of b_w does not produce any change in the overall response.

The peak NSM shear strength contribution $V_{f,k}^{\max}$ presents, with respect to either of the CFRP strip's cross-section dimensions (a_f or b_f), a three-phases trend (Fig. 4e-f). In the first phase ($a_f \le 1.5\ mm$ or $b_f \le 8\ mm$), the prevalent failure mode is tensile rupture of the strips and $V_{f,k}^{\max}$ increases almost linearly by increasing either a_f or b_f. In fact, after a soon and shallow concrete fracture, most of the strips crossing the CDC rupture due to their reduced cross-section area. In the intermediate phase ($1.5 < a_f \le 4.5\ mm$ or $8 < b_f \le 12\ mm$, where 1 *mm* = 0.0394 *in*), the prevailing failure mode is mixed-shallow-semi-cone-plus-debonding and $V_{f,k}^{\max}$ increases, by increasing either a_f or b_f, with a gradually decreasing rate. By increasing either of the strip's cross-sectional dimensions, after an initial and deeper concrete fracture, the remaining resisting bond lengths, even if relatively shorter with respect to the first phase, can mobilize bond at a higher extent, which means that a larger percentage of the peak force they would be able to transfer through bond $V_{fi}^{bd,\max}$ can actually be attained due to the larger tensile rupture capacity V_f^{tr}. In the third phase ($a_f > 4.5\ mm$ or $b_f > 12\ mm$), the commanding failure mode is concrete semi-conical fracture since concrete fracture becomes progressively deeper up

to reaching the free extremities of the available bond lengths and $V_{f,k}^{\max}$ is almost independent of the value assumed by either of the cross-sectional dimensions.

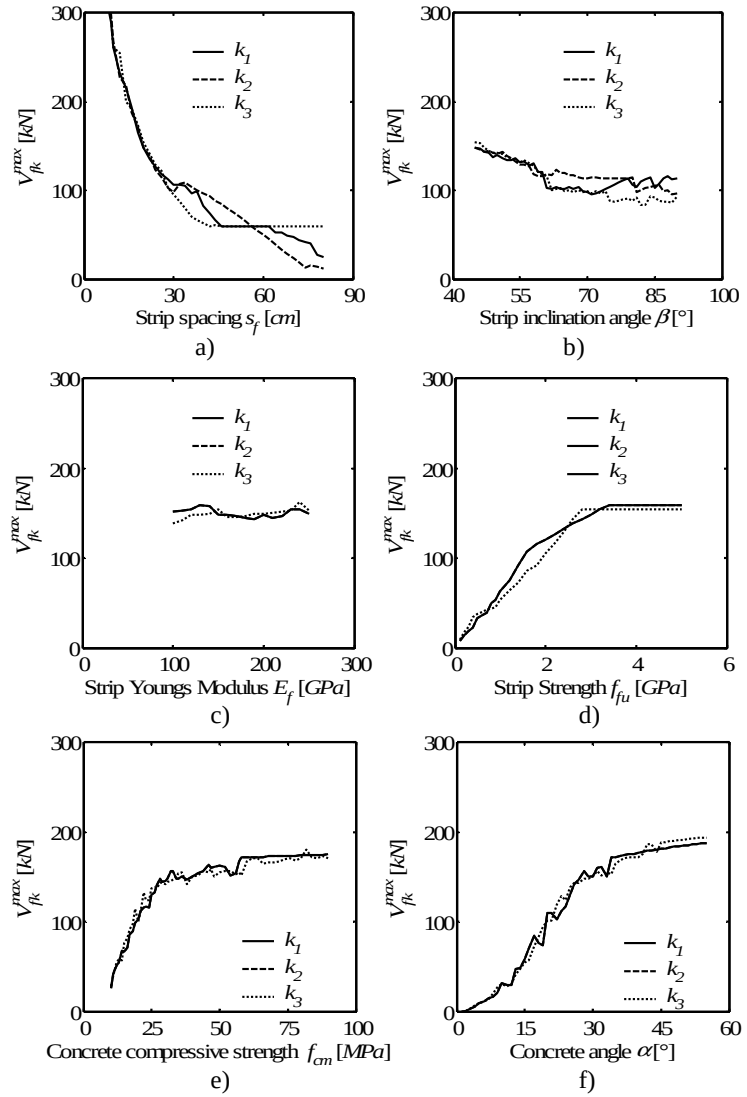

Figure 5 — Influence on the peak NSM shear strength contribution $V_{f,k}^{\max}$ of: a) strips' spacing s_f; b) strips' inclination angle β; c) strip's Young's Modulus E_f; d) strip's strength f_{fu}; e) concrete compressive strength f_{cm} and f) of the concrete fracture angle α (1 *mm* = 0.0394 *in* - 1 *N* = 0.2248 *lb*).

However, for very large values of either of the strip cross-section dimensions, the model progressively loses accuracy underestimating the concrete fracture capacity since the approximation of the concrete fracture surface as a semi-cone whose axis lies on the web face may no longer be acceptable.

By increasing the spacing s_f between adjacent strips, their contribution to the peak NSM shear strength significantly decreases (Fig. 5a) since the number of strips effectively crossing the CDC decreases in turn. For very short values of s_f, due to the high interaction between adjacent strips (Bianco *et al.* 2010), concrete tensile fracture capacity is very low so that concrete fracture is relatively deeper. The strips characterized by the shorter available bond lengths fail since concrete fracture reaches their free extremity, the ones characterized by an average value of available bond length undergo a mixed-shallow-semi-cone-plus-debonding failure and the central, longer ones, rupture. For increasing values of s_f, concrete semi-conical fracture becomes progressively shallower and the strips characterized by the shorter available bond lengths fail due to mixed-shallow-semi-cone-plus-debonding failure and the central ones rupture.

By further increasing s_f, the number of strips crossing the CDC progressively reduces. For the cases of spacing larger than 500 *mm*, the number of strips effectively crossing the CDC varies between two and one. For these cases, the strips generally undergo an initial shallow concrete fracture followed by loss of bond while the central ones, or the only one in the case of one strip only crossing the CDC, ruptures.

By increasing the value of the inclination of the strips with respect to the beam axis β (Fig. 1a-b), the peak NSM shear strength contribution decreases (Fig. 5b) mainly because, other parameters being the same, both the number of strips effectively crossing the CDC and their initial available bond lengths decrease.

The strip's Young's Modulus E_f has, on the whole and for the values assumed in the present study, a negligible influence on $V_{f,k}^{\max}$ (Fig. 5c). In fact, since the value of E_f mainly influences the value of the necessary bond transfer length $L_{tr}^{bd}(\delta_{Li})$ (Bianco 2008), it ends up influencing, in the initial load steps, the penetration depth of concrete fracture inside the web core. Nevertheless, having herein assumed a very low value of the increment of the CDC opening angle $\dot{\gamma}$, although different values of E_f could imply a different penetration depth of concrete fracture in the initial load steps, the last values assumed by the resisting bond lengths L_{Rfi} result, altogether, almost equal. Therefore, since similar values of L_{Rfi} can mobilize a maximum value of bond force $V_{fi}^{bd,\max}$ which is practically the same, E_f only negligibly influences the peak NSM shear strength contribution $V_{f,k}^{\max}$.

The trend of the peak NSM shear strength contribution $V_{f,k}^{\max}$ with respect to the strip tensile strength f_{fu} shows two phases separated by an almost clear-cut turning point approximately in correspondence of the value of 3.0 *GPa* (1000 *psi* = 6.9 *MPa*).

(Fig. 5d). For values of f_{fu} smaller than 3.0 *GPa*, the ultimate behavior is governed by the prevalent rupture of the strips. In fact, after the initial concrete fracture, which generally occurs around all of them, most of the strips fail by rupture. For increasing values of f_{fu}, after the initial concrete fracture, due to the increased value of the strip tensile capacity V_f^{tr}, the last values assumed by the strips resisting bond lengths can mobilize a progressively larger percentage of their bond-capacity $V_{fi}^{bd,max}$ and the number of strips that undergo rupture progressively reduces to the central ones only. For values of f_{fu} approaching 3.0 *GPa*, due to the increased strip tensile capacity, the last values assumed by the strips resisting bond lengths can attain their entire bond-capacity $V_{fi}^{bd,max}$ without rupturing since $V_{fi}^{bd,\max} < V_f^{tr}$. Since f_{fu} does not affect the mechanics of bond, *i.e.* it has no influence on either $L_{tr,fi}^{bd}(\delta_{Li})$ or $V_{fi}^{bd,\max}$ as long as this latter is smaller than V_f^{tr}, for values of f_{fu} larger than 3.0 *GPa*, strips no longer rupture and the ultimate state, characterized by mixed-shallow-semi-cone-plus-debonding for all of the strips, remains exactly the same regardless of the value assumed by f_{fu}.

The variation of $V_{f,k}^{\max}$ with respect to concrete mechanical properties f_{cm} and α presents a nonlinear trend (Figs. 5e-f) in which three successive linear branches, mutually connected by gradually varying stretches, can be singled out. In the first phase ($\alpha \le 10^o$ and $f_{cm} \le 10$ *MPa*, not represented in Fig. 12e since concrete is not *structural*), due to the fact that concrete mechanical properties are very low, concrete fracture penetrates very deep inside the core of the beam web up to quickly reaching all of the strips' free extremity. In this first phase, in which concrete fracture is the prevailing failure mode, $V_{f,k}^{\max}$ is very low and increases linearly for increasing values of either f_{cm} or α. By further increasing f_{cm} or α, concrete fracture becomes progressively shallower so that: a) the resisting bond lengths that result after the last concrete fracture are longer and b) the number of strips, in correspondence of which concrete fracture reaches the free extremity, reduces to the shorter ones only while the longer ones undergo an abrupt reduction of their resisting bond length. In the second phase ($10^o < \alpha \le 30^o$ and $10 < f_{cm} \le 30$ *MPa*) most of the strips fail due to mixed shallow-semi-cone-plus-debonding so that the last values of the resisting bond lengths and in turn, the maximum value of force they can transfer by bond $V_{fi}^{bd,\max}$, increase. Thus the peak NSM shear strength contribution $V_{f,k}^{\max}$ increases according to a linear trend that presents an inclination larger than the one characterizing the first phase and much closer to the one characterizing the relationship between $V_{fi}^{bd,\max}$ and L_{Rfi} (Bianco 2008). In the second intermediate phase ($30^o < \alpha \le 40^o$ and $30 < f_{cm} \le 60$ *MPa*), concrete fracture continues to become shallower and the last values of the resisting bond lengths progressively become long enough to allow the transfer, through bond stresses, of a force large enough

to equal the strip rupture capacity V_f^{tr}. Therefore, in this intermediate phase, by increasing f_{cm} or α, central strips start to rupture and $V_{f,k}^{\max}$ increases by a progressively decreasing rate. In the third and last phase ($\alpha > 40^o$ and $f_{cm} > 60\ MPa$), even if concrete fracture becomes shallower and shallower and the last values of the resisting bond lengths larger, $V_{f,k}^{\max}$ does not further increase since the central strips, which substantially contribute to the peak value, rupture for a certain value of γ. Therefore, in this last phase, $V_{f,k}^{\max}$ is practically independent of the value assumed by either f_{cm} or α.

The parameter τ_0 has a negligible influence on the peak NSM shear strength contribution $V_{f,k}^{\max}$ (Fig. 7a). For the range of values herein adopted (Table 1), that are deemed physically reasonable, τ_0 only slightly influences the extent to which the initial concrete fracture around each strip penetrates inside the web core (Bianco 2008). In fact, the larger τ_0, the slightly shallower the concrete fracture and, in turn, the slightly larger the last values of the resisting bond lengths. Nevertheless, at those slightly larger values of L_{Rfi} does not correspond an appreciable variation of $V_{f,k}^{\max}$ since, even if the peak force these latter can transfer by bond $V_{fi}^{bd,\max}$ is larger, it can not be entirely attained. In fact the central strips, which mainly contribute to the peak NSM shear strength contribution $V_{f,k}^{\max}$, prematurely fail by rupture.

The peak bond strength τ_1 has, despite a fluctuation around an average value, a marginal influence on $V_{f,k}^{\max}$ (Fig. 6b). Since for smaller values of τ_1, the necessary bond transfer length $L_{tr}(\delta_{Li})$ is larger (Bianco 2008), in the very first t_n steps of the loading process $\gamma(t_n)$, the resulting imposed end slip $\delta_{Li}[\gamma(t_n)]$ and the force originating in the loaded end being the same, concrete semi-conical fracture is deeper. Nonetheless, concrete fracture stops progressing inwards relatively much earlier since the vertices of the hypothetical concrete semi-conical fracture surfaces reach, in the following steps, such depths that the corresponding concrete fracture strength $V_{fi}^{cf}\left(X_i^l\right)$ is large enough to prevent further fracture. It results that the latest semi-conical concrete fractures are shallower with respect to the case of a larger τ_1 and that the remaining resisting bond lengths are relatively longer. On the contrary, in the case of a larger value of τ_1, concrete fracture penetrates deeper inside the web core and the resulting latest resisting bond lengths are shorter. Nevertheless, even if different values of the last resisting bond lengths L_{Rfi}, for different values of τ_1, would be capable of attaining different values of $V_{fi}^{bd,\max}$ (Bianco 2008), these latter are always larger than V_f^{tr}, regardless of the value assumed by τ_1, so that they can not be attained since strips rupture beforehand.

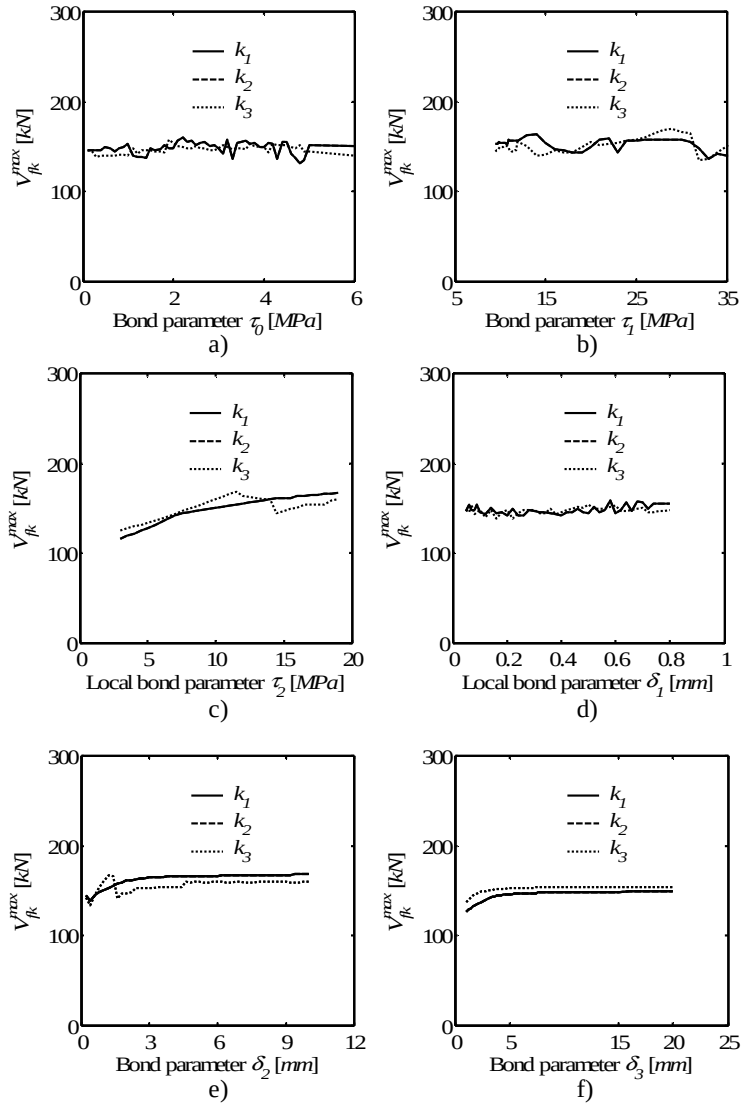

Figure 6 — Influence on the peak NSM shear strength contribution $V_{f,k}^{\max}$ of the local bond stress slip relationship parameters: a) τ_0, b) τ_1, c) τ_2, d) δ_1, e) δ_2 and f) δ_3 (1 *mm* = 0.0394 *in* - 1 *N* = 0.2248 *lb* - 1000 *psi* = 6.9 *MPa*).).

Thus, the peak of the shear strength contribution provided by a system of NSM FRP strips $V_{f,k}^{\max}$ does not appreciably vary by varying τ_1 since, in correspondence of the γ for which $V_{f,k}^{\max}$ is attained, the central and longer strips prematurely rupture.

The peak shear strength contribution provided by a system of NSM FRP strips $V_{f,k}^{\max}$ shows, by increasing τ_2 and for the values herein assumed for the other parameters, a pseudo bi-linear trend (Bianco 2008) with a not clear-cut division between the two pseudo straight lines. Since an increase of τ_2 only yields a decrease of the necessary bond transfer length $L_{tr}^{bd}(\delta_{Li})$ for values of the imposed end slip larger than approximately 2.0 *mm* (Bianco 2008), it does not produce any variation in the penetration depth of concrete fracture that generally occurs in the first load steps in which the values of imposed end slip δ_{Li} are low. Thus, the resisting bond lengths that remain after the last semi-conical fracture has occurred around each of the strips effectively crossing the CDC, have almost the same values regardless of the value of τ_2. However, for a generic value of the resisting bond length, by increasing τ_2, the peak force transmissible by bond $V_{fi}^{bd,\max}$ increases, (Bianco 2008). Along the first of those branches ($\tau_2 \le 12.5\,MPa$ - 1000 *psi* = 6.9 *MPa*), by increasing τ_2, $V_{f,k}^{\max}$ slightly increases while in the second branch ($\tau_2 > 12.5\,MPa$) $V_{f,k}^{\max}$ is almost constant. Along the first branch, at attainment of $V_{f,k}^{\max}$, the central strips, characterized by the larger values of L_{Rfi}, manage to attain their peak bond-transferred force $V_{fi}^{bd,\max}$ while in the second branch, in correspondence of the peak $V_{f,k}^{\max}$, the central strips undergo tensile rupture without being able of mobilizing the whole bond force they are capable to transfer $V_{fi}^{bd,\max}$. The slight increase of $V_{f,k}^{\max}$ in the second branch is due to the contribution of the lateral strips that, even if undergo mixed-shallow-semi-cone-plus-debonding, in correspondence of the attainment of $V_{f,k}^{\max}$ still have a resisting bond length large enough to register an increase of bond transferred force for increasing values of τ_2.

The parameter δ_1 has, for the values of the various parameters herein assumed, a negligible influence on the peak NSM shear strength contribution (Fig. 7d). By increasing δ_1, the bond results softer in the sense that, for an equal value of the imposed end slip δ_{Li}, the necessary transfer length is longer (Bianco 2008). For a larger value of δ_1 and for an equal value of δ_{Li}, concrete fracture in the first load steps is relatively deeper but it stops progressing inwards much earlier. It follows that, the smaller the value of δ_1, the deeper the concrete fracture penetration inside the web core and in turn, the smaller the latest resisting bond lengths. On the contrary, for larger values of δ_1, the latest resisting bond lengths are longer. Nonetheless, even if for different values of δ_1 the last values of the resisting bond lengths are different, and due to that, would be capable of

providing a different value of the maximum contribution $V_{fi}^{bd,\max}$ (Bianco 2008), this latter can not be entirely attained since the strips rupture for a smaller value and $V_{f,k}^{\max}$ is approximately the same.

The slip values δ_2 and δ_3 have a similar influence, though marginal, on the peak NSM shear strength contribution $V_{f,k}^{\max}$ (Fig. 7e-f). By increasing δ_2 or δ_3, the necessary transfer lengths, the imposed end slip being the same, decrease but only for large values of the imposed end slip (Bianco 2008). On the contrary, for very small values of δ_{Li}, which are those corresponding to the first load steps in which generally concrete fractures, the necessary transfer lengths are not affected by a variation in the value of either δ_2 or δ_3. It follows that, regardless of the value assumed for δ_2 or δ_3, the concrete semi-conical fracture has the same depth and, consequently, the latest values assumed by the resisting bond lengths do not vary by varying δ_2 or δ_3. Anyway, by increasing δ_2 or δ_3, the maximum bond transferrable force $V_{fi}^{bd,\max}$ varies as function of the value of the resisting bond length (Bianco 2008). Thus, by increasing δ_2 or δ_3 (Fig. 7e-f), an increase of $V_{f,k}^{\max}$ can be noticed as long as the maximum force transferrable by bond $V_{fi}^{bd,\max}$ is smaller than the strip tensile rupture capacity V_f^{tr}. From the value of δ_2 (or δ_3) in correspondence of which the central strips start to rupture, $V_{f,k}^{\max}$ does not further increase by increasing δ_2 (or δ_3).

CONCLUSIONS

The main features of a mechanical model that was recently developed to predict the NSM FRP strips shear strength contribution to a RC beam were presented. That model was first appraised on the basis of available experimental results and then was applied to evaluate the influence of each of the intervening parameters on the shear strength contribution provided to a RC beam by a system of NSM strips.

The behavior of a system of NSM FRP strips contributing to the shear strength of a RC beam is extremely complex due to: 1) interaction among adjacent strips, 2) interaction among all the possible failure modes, 3) complicate geometry and 4) asymmetric distribution of imposed end slips. For these reasons, the dependency of the peak NSM FRP strips shear strength contribution on most of the intervening parameters is extremely non-linear.

From the results of the parametric studies it arises that a variation in each of the parameters analyzed yields a gradual variation of both the prevailing ultimate behavior and configuration assumed by the system of NSM FRP strips. Nonetheless, the threshold values of the parameters that mark the passage from one behavior to the other can not be taken as universally valid but they are valid relatively to the set of values assumed for the other parameters. However, the outcomes of the studies presented are very useful to better understand the relative influence of the various input parameters on the ultimate behavior of the system of NSM FRP strips.

Since the very first steps of the loading process, concrete fractures, in the shape of concentric successive semi-cones, around each of the strips. The resulting envelope fracture surface, starting from the CDC plane, progressively penetrates inside the web core reducing the strips' resisting bond lengths. The lower the concrete mechanical properties, the deeper concrete fractures.
A variation in the parameters defining the local bond stress-slip relationship can be felt, in terms of peak shear strength contribution, only as long as the last values assumed by the strips' resisting bond lengths are such as to transfer, through bond, a maximum force that is lower than the strip rupture capacity.

ACKNOWLEDGEMENTS

The authors of the present work wish to acknowledge the support provided by the "Empreiteiros Casais", S&P®, degussa® Portugal, and Secil (Unibetão, Braga). The study reported in this paper forms a part of the research program "CUTINEMO" supported by FCT, PTDC/ECM/73099/2006. Also, this work was carried out under the auspices of the Italian DPC-ReLuis Project (repertory n. 540), Research Line 8, whose financial support is greatly appreciated.

REFERENCES

Bianco, V., Barros, J.A.O., Monti, G., (2006). "Shear Strengthening of RC beams by means of NSM laminates: experimental evidence and predictive models", Technical report 06-DEC/E-18, Dep. Civil Eng., School Eng. University of Minho, Guimarães-Portugal.

Bianco, V., Barros, J.A.O., Monti, G., (2007a). "A new approach for modeling the NSM shear strengthening contribution in reinforced concrete beams", FRPRCS-8, University of Patras, Greece,16-18 July, ID 8-12.

Bianco, V., Barros, J.A.O., Monti, G., (2007b). "Shear Strengthening of RC beams by means of NSM strips: a proposal for modeling debonding", Technical report 07-DEC/E-29, Dep. Civil Eng., School Eng. University of Minho, Guimarães- Portugal.

Bianco, V., (2008). "Shear Strengthening of RC beams by means of NSM FRP strips: experimental evidence and analytical modeling", PhD Thesis, Dept. of Structural Engrg. and Geotechnics, Sapienza University of Rome, Italy, submitted on December 2008.

Bianco, V., Barros, J.A.O., Monti, G., (2009a). "Three dimensional mechanical model for simulating the NSM FRP strips shear strength contribution to RC beams", Engineering Structures, 31(4), April 2009, 815-826.

Bianco, V., Barros, J.A.O., Monti, G., (2009b). "Bond Model of NSM FRP strips in the context of the Shear Strengthening of RC beams", ASCE Journal of Structural Engineering, 135(6), June 2009.

Bianco, V., Barros, J.A.O., Monti, G., (2010). “New approach for modeling the contribution of NSM FRP strips for shear strengthening of RC beams”, ASCE Journal of Composites for Construction, 14(1), January/February 2010.

CEB-FIP Model Code 90, (1993) Bulletin d’Information N° 213/214, Final version printed by Th. Telford, London, (1993; ISBN 0-7277-1696-4; 460 pages)

Dias, S.J.E., Bianco, V., Barros, J.A.O., Monti, G., (2007). “Low strength concrete T cross section RC beams strengthened in shear by NSM technique”, Workshop-Materiali ed Approcci Innovativi per il Progetto in Zona Sismica e la Mitigazione della Vulnerabilità delle Strutture, University of Salerno, Italy, 12-13 February.

Dias, S.J.E. and Barros, J.A.O., (2008). “Shear Strengthening of T Cross Section Reinforced Concrete Beams by Near Surface Mounted Technique”, Journal of Composites for Construction, ASCE, Vol. 12, No. 3, pp. 300-311.

Mohammed Ali, M.S., Oehlers, D.J., Seracino, R. (2006). “Vertical shear interaction model between external FRP transverse plates and internal stirrups”, Engineering Structures 28, 381-389.

Mohammed Ali, M.S., Oehlers, D.J., Griffith, M.C., Seracino, R. (2007). “Interfacial stress transfer of near surface-mounted FRP-to-concrete joints”, Engineering Structures 30, 1861-1868.

Rizzo, A. and De Lorenzis, L., (2009) “Behaviour and capacity of Rc beams strengthened in shear with NSM FRP reinforcement”, Construction and Building Materials, Vol. 3, n. 4, April 2009, 1555-1567.

Sekulic, A., Curnier, A., (2006). “An original epoxy-stamp on glass-disc specimen exhibiting stable debonding for identifying adhesive properties between glass and epoxy”, International Journal of Adhesion and Adhesives, Vol. 27, pp. 611-620.

Sena-Cruz, J.M. (2004). “Strengthening of concrete structures with near-surface mounted CFRP laminate strips” PhD Thesis, Department of Civil Engineering, University of Minho, Guimarães-Portugal.

Sena-Cruz, J.M., Barros, J.A.O., (2004). “Bond between near-surface mounted CFRP laminate strips and concrete”, Journal of Composites for Construction, ASCE, Vol. 8, No. 6, pp. 519-527.

Yuan, H., Teng, J.G., Seracino, R., Wu, Z.S., Yao, J. (2004). “Full-range behavior of FRP-to-concrete bonded joints”, Engineering Structures, 26, 553-565.

Zhai, L.L., Ling, G.P., Wang, Y.W., (2008). “Effect of nano-Al_2O_3 on adhesion strength of epoxy adhesive and steel”, International Journal of Adhesion and Adhesives, Vol. 28, No. 1-2, pp. 23-28.